QUANTIFYING THE PERFORMANCE OF A TOP-DOWN

NATURAL VENTILATION WINDCATCHER™

Benjamin M. Jones[a,b] and Ray Kirby[b,*]

[a]Monodraught Ltd.

Halifax House, Halifax Road, Cressex Business Park

High Wycombe, Buckinghamshire, HP12 3SE

[b]School of Engineering and Design,

Mechanical Engineering,

Brunel University, Uxbridge, Middlesex, UB8 3PH, UK.

ray.kirby@brunel.ac.uk

* Corresponding author.

Address for correspondence:

Dr. Ray Kirby,

School of Engineering and Design,

Mechanical Engineering,

Brunel University,

Uxbridge,

Middlesex, UB8 3PH.

Email: ray.kirby@brunel.ac.uk

Tel: +44 (0)1895 266687

Fax: +44 (0)1895 256392

Abstract

Estimating the performance of a natural ventilation system is very important if one is to correctly size the system for a particular application. Estimating the performance of a Windcatcher™ is complicated by the complex flow patterns that occur during the top-down ventilation process. Methods for predicting Windcatcher™ performance can currently be separated into simplistic analytic methods such as the envelope flow model and the use of complex and time consuming numerical methods such as CFD. This article presents an alternative semi-empirical approach in which a detailed analytic model makes use of experimental data published in the literature for 500 mm square Windcatchers™, in order to provide a fast but accurate estimate of Windcatcher™ performance. Included in the model are buoyancy effects, the effect of changes in wind speed and direction, as well as the treatment of sealed and unsealed rooms. The semi-empirical predictions obtained are shown to compare well with measured data and CFD predictions, and air buoyancy is shown only to be significant at relatively low flow velocities. In addition, a very simple algorithm is proposed for quantifying the air flow rates from a room induced by a Windcatcher™ in the absence of buoyancy effects.

Keywords: Natural Ventilation, Windcatcher™, Analytic Model, Buoyancy

1. Introduction

A Windcatcher™† is a top-down, roof mounted, omni-directional device used for naturally ventilating buildings. The Windcatcher™ protrudes out from a roof and works by channelling air though a series of louvers into a room under the action of wind pressure, and simultaneously drawing air out of the room by virtue of a low pressure region created downstream of the Windcatcher™. The Windcatcher™ concept has been around for centuries and is commonplace in the Middle East [1, 2]. This concept has been applied commercially in the UK for at least 30 years, see for example the review of Windcatchers™ and other related wind driven devices by Khan *et al.* [3]. The cross-section of the Windcatcher™ may be any shape, although it is important to try and maximise the pressure drops on the leeward side and so current commercial designs are either circular or rectangular. Experimental studies have shown, however, that a Windcatcher™ of rectangular cross-section outperforms other designs, see for example Refs. [4] and [5]. For a rectangular Windcatcher™, the cross-section is normally split up into four quadrants so that one or more quadrants act as supply ducts to a room and the remaining quadrants act as extract ducts. The key indicator of performance for a Windcatcher™ is the rate at which fresh air is delivered into the room and the rate at which stale air is extracted. Accordingly, it is very important to be able to predict ventilation rates prior to choosing the appropriate size of a Windcatcher™ for a particular building. This article addresses this issue by developing a simple semi-empirical model suitable for estimating Windcatcher™ performance as a function of wind velocity and cross-sectional area.

†Windcatcher™ is a proprietary product of Monodraught Ltd.

It is common to predict natural ventilation flow rates using simple envelope flow models, see for example Refs. [6-10]. A major factor that influences the performance of a natural ventilation system is the losses incurred as the air passes through an opening. For envelope flow models it is normally assumed that these losses can be modelled using an equivalent coefficient of discharge, and values similar to those measured for orifice plates are commonly used [6, 9]. However, a Windcatcher™ represents a far more complex opening than, say, a window and such an approach is unlikely to capture the true performance of a Windcatcher™ over a range of parameters. Therefore, in order to realise a more accurate understanding of the energy losses inside a Windcatcher™ it is necessary to study the air flow in more detail. Experimental and theoretical investigations into Windcatcher™ performance have been reported in the literature, although data on Windcatchers™ is not as prevalent as that seen for other types of natural ventilation. The measurement of Windcatcher™ performance has generally been restricted to laboratory conditions and very few studies have examined performance *in situ*. For example, Elmualim and Awbi [5], Parker and Teekeram [11], and Elmulalim [12] all used a wind tunnel to measure the performance of a square Windcatcher™ divided into four quadrants and connected to a sealed room; later, Su *et al.* [13] performed similar wind tunnel tests but for circular Windcatchers™. Parker and Teekeram focussed on measuring the average coefficient of pressure (C_p) over each face of the Windcatcher™ for wind of normal incidence. Elmualim [12] also measured C_p values, but extended the study to wind incident at different angles in order to build up a more general picture of a Windcatcher's™ performance. The experimental data reported by Elmualim [12] is based on measurements taken using only two pressure tappings placed on the centre line of each Windcatcher™ face, which may introduce further errors and is significantly fewer in number than the pressure tappings used by Parker and Teekeram [11]. Kirk and

5

Kolokotroni [14] also measured the performance of rectangular Windcatchers™, but chose to measure the ventilation flow rates for multiple Windcatchers™ operating *in situ*. Kirk and Kolokotroni measured the decay of tracer gas in order to estimate ventilation rates and for an office environment they observed a linear relationship between extract volume flow rate and the incident wind velocity. A linear relationship was also observed by Shea *et al.* [15], who measured a net flow out of the Windcatcher™ indicating that there is air infiltration into the room to compensate for the mass shortfall.

The values measured for C_p clearly demonstrate the action of the Windcatcher™ in that those quadrants with positive values of C_p act as supply ducts, whereas those with negative values act as extract ducts. This is also confirmed by observations taken using smoke tests, see for example the measurements of Elmualim and Awbi [5]. To corroborate laboratory measurements, Elmualim and Awbi [5] developed a CFD model for both circular and rectangular Windcatchers™, and for the windward quadrant under normal incidence good agreement between predicted and measured C_p values was observed for the rectangular Windcatcher™. However, a comparison between prediction and measurement for the leeward faces is less successful, although this is, perhaps, not surprising given the complex and highly turbulent nature of the air flow around a typical Windcatcher™. Whilst the measured C_p values are important in dictating the magnitude and direction of the flow velocities into and out of a room, they do not on their own quantify the ventilation rates. Here, ventilation rates also depend on the losses within the Windcatcher™, which must be quantified before a complete picture of Windcatcher™ performance can be realised. The ventilation rates for a 500 mm square Windcatcher™ were measured by Elmualim and Awbi [5] under controlled conditions in a wind tunnel. Later, Elmualim [12] used CFD to predict ventilation rates in a square Windcatcher™, although only

limited agreement with measured data is observed. Li and Mak [16] also used CFD to examine the performance of a 500 mm square Windcatcher™ and demonstrated good agreement with Elmulaim and Awbi's [5] data, although this is limited to overall ventilation rates. Recently, Hughes and Ghani [17] used CFD to calculate net flow rates through a 1000 mm square Windcatcher™, and by normalising their results they were able to obtain predictions that agreed to within 20% of those generated by Elmualim [12]; see also an earlier CFD study by the same authors [18].

Whilst CFD models have been shown to be partially successful in capturing the performance of a Windcatcher™, the difficulty of using CFD to generate predictions covering a wide range of parameters, as well as the time taken to generate and solve these models, means that CFD is not so useful as an iterative design tool. Moreover, the very function of a Windcatcher™ depends on high levels of turbulence and early boundary layer separation, an area that not surprisingly causes CFD problems. Accordingly, it appears to be sensible to investigate an analytic approach with a view to developing simple algorithms based on the use of empirical data to estimate the losses due to turbulence. To this end, Elmualim [12] used a so-called explicit model in order to estimate Windcatcher™ performance and represented the losses within the Windcatcher™ using an equivalent coefficient of discharge. This approach is very similar to the envelope flow model described by Etheridge [7], although good agreement with experiment is observed only under limited conditions. Moreover, the method uses two heuristic constants that appear to bear very little relation to the Windcatcher™ itself and it is not clear why certain values were chosen, nor how one should go about identifying these values for different Windcatcher™ designs. Accordingly, there is a clear need for a simple analytic model from which Windcatcher™ performance can be quickly and reliably estimated. This

article addresses this need by developing an analytic model that explicitly includes experimental data for the Windcatcher™ as part of the modelling methodology, as well as adding other phenomena such as buoyancy. Here, experimental data is used to quantify the losses in the Windcatcher™ rather than using CFD or heuristic constants. Furthermore, the model is extended to address both sealed and unsealed rooms and will also deliver results for wind incident at two different angles, something that is omitted in the explicit model of Elmualim [12]. Accordingly, in Section 2 that follows an analytic model is developed based on conservation of energy and mass. Experimental data reported in the literature and obtained under controlled laboratory conditions is then used to identify appropriate C_p values in Section 3; by comparing prediction and experiment appropriate loss factors are also calculated and a semi-empirical model formulated. In Section 4 the semi-empirical predictions are compared against other data available in the literature and a very simple relationship between Windcatcher™ ventilation rates, incident wind velocity and Windcatcher™ area is presented.

2. Analytic Model

A Windcatcher™ is normally either rectangular or circular in cross-section, although a Windcatcher™ of rectangular cross-section is known to significantly outperform one of circular cross-section [5] and so the analysis that follows is restricted to rectangular cross-sections. The cross-section is assumed to be divided up into four quadrants, where each quadrant contains louvers at the top and dampers plus a grill at the bottom, see Fig. 1. The Windcatcher™ experiences wind of velocity u_w incident at an angle of θ degrees, see Fig.

1a. The Windcatcher™ has cross-sectional dimensions $d_1 \times d_2$; the length of the louver section is L_I and the length of the section from the louvers to the bottom is L.

To model the performance of a Windcatcher™ conservation of energy and mass are enforced using a method similar to that reported by Etheridge and Sandberg [6], and CIBSE [8]. In the analysis that follows, the wind is assumed to have zero angle of incidence ($\theta = 0°$) as this will simplify the discussion; however, a value of $\theta = 45°$ will be included in Section 3. For a quadrant that faces into the wind, flow will be from the outside into the room and here conservation of energy yields [6],

$$\Delta p_{\text{in}} = p_E - p_I - \Delta \rho g \, z_I + p_w, \tag{1}$$

where p_E and p_I are the external and internal pressures, respectively, and Δp_{in} is the pressure drop over the Windcatcher™ quadrant (assuming that all losses between the room and the surroundings are attributable solely to the Windcatcher™). In addition, $\Delta \rho$ denotes the change in air density between the room and the surroundings, z_I denotes the height of the entrance to the Windcatcher™ from the room, relative to the lower surface of the room, and p_w denotes the pressure generated by the wind. Similarly, for a quadrant in which air travels from the room to the surroundings,

$$\Delta p_{\text{out}} = p_I - p_E + \Delta \rho g \, z_E - p_w, \tag{2}$$

where Δp_{out} is the pressure drop over the outlet quadrant. In general, the pressure generated by the action of the wind over the face of a Windcatcher™ quadrant may be

9

related to the velocity of the air flowing into or out of the quadrant by use of the coefficient of pressure C_p, which is defined as [6]

$$C_p = \frac{\Delta p}{\rho_E u_w^2 / 2}.$$

(3)

Here, Δp is the difference between the static pressure on the face of the Windcatcher™ (p_w) and a reference pressure. Thus, for air flow from the surroundings into the room (an "inlet" quadrant) Eq. (1) may be re-written as [6]

$$\Delta p_{in} = \frac{1}{2} \rho_E u_w^2 C_p - g z_I (\rho_E - \rho_I) - p_I,$$

(4)

where $\Delta \rho = \rho_E - \rho_I$ and the reference pressure is assumed to be atmospheric. Equation (4) also assumes that the air velocity in the room is negligible and changes in density caused by the variation of pressure with height may be neglected. Similarly, for an outlet quadrant

$$\Delta p_{out} = p_I - g z_E (\rho_I - \rho_E) - \frac{1}{2} \rho_E u_w^2 C_p.$$

(5)

The change in density that appears in Eqs. (4) and (5) is assumed here to be due solely to temperature changes and, following Etheridge and Sandberg [6],

$$\Delta p_{in} = \frac{1}{2} \rho_E u_w^2 C_p - \frac{g z_I p_E}{R} \left(\frac{1}{T_E} - \frac{1}{T_I} \right) - p_I$$

(6)

and

$$\Delta p_{\text{out}} = p_I - \frac{g z_E p_E}{R} \left(\frac{1}{T_I} - \frac{1}{T_E} \right) - \frac{1}{2} \rho_E u_w^2 C_p . \tag{7}$$

Here T denotes temperature and R is the specific gas constant for air. The pressure drops Δp_{in} and Δp_{out} represent the losses imparted by the Windcatcher™ and these losses may be expressed in a number of ways, for example using a standard loss coefficient (see CIBSE, [8]). However, the Windcatcher™ contains many different elements and it is desirable here to gain an appreciation of how each element impacts on Windcatcher™ performance and so the losses are expressed in terms of a loss coefficient K, where in general

$$K_{\text{in, out}} = \frac{\Delta p_{\text{in, out}}}{\rho u^2 / 2} . \tag{8}$$

This allows Eqs. (6) and (7) to be re-written to give

$$\frac{1}{2} \overline{\rho} u_{\text{in}}^2 K_{\text{in}} = \frac{1}{2} \rho_E u_w^2 C_p - \frac{g z_I p_E}{R} \left(\frac{1}{T_E} - \frac{1}{T_I} \right) - p_I \tag{9}$$

and

$$\frac{1}{2} \overline{\rho} u_{\text{out}}^2 K_{\text{out}} = p_I - \frac{g z_E p_E}{R} \left(\frac{1}{T_I} - \frac{1}{T_E} \right) - \frac{1}{2} \rho_E u_w^2 C_p . \tag{10}$$

Here, u_{in} and u_{out} represent the velocity inside the quadrant of an inlet and outlet duct, respectively, and $\overline{\rho}$ is an average value for density over the length of the quadrant.

For $\theta = 0°$, we may assume that one quadrant acts as an inlet [quadrant (1)] and three quadrants act as an outlet, where quadrants (2) and (3) are assumed to be identical, see for example the experimental data of Elmualim [12]. After re-arranging, conservation of energy for the inlet and outlet quadrants may be written as

$$\frac{1}{2}\overline{\rho}u_1^2 K_1 = \frac{1}{2}\rho_E u_w^2 C_{p_1} - \frac{gz_I p_E}{R}\left(\frac{1}{T_E} - \frac{1}{T_I}\right) - p_I, \tag{11}$$

$$\frac{1}{2}\overline{\rho}u_2^2 K_2 = p_I + \frac{gz_E p_E}{R}\left(\frac{1}{T_E} - \frac{1}{T_I}\right) - \frac{1}{2}\rho_E u_w^2 C_{p_2} \tag{12}$$

and

$$\frac{1}{2}\overline{\rho}u_4^2 K_4 = p_I + \frac{gz_E p_E}{R}\left(\frac{1}{T_E} - \frac{1}{T_I}\right) - \frac{1}{2}\rho_E u_w^2 C_{p_4} \tag{13}$$

assuming that the external temperature is the same for each quadrant.

To solve Eqs. (11)-(13) it is necessary also to enforce mass continuity, which will depend on the conditions assumed inside the room. Here, there are two limiting cases (i) a room in which air exchange with the surroundings is permitted, and (ii) a room that is perfectly sealed. Both scenarios will be considered here, with a sealed room to be studied first.

2.1. Sealed room

For a sealed room, mass continuity for $\theta = 0^0$ in which air flows in through quadrant 1 and out through quadrants 2, 3 and 4, gives

$$\dot{Q}_1 = 2\dot{Q}_2 + \dot{Q}_4, \tag{14}$$

where $\dot{Q}$ is the volume flow rate inside the Windcatcher™ and quadrants (2) and (3) are assumed to be identical. Here, the density (and hence temperature) of the air inside each quadrant is assumed to be equal in order to be consistent with the average values for density used previously for the energy equation. Writing Eq. (15) in terms of the velocity in each quadrant yields,

$$u_1 A_1 = 2u_2 A_2 + u_4 A_4 \qquad (15)$$

where A is the area of a quadrant. Equations (11)-(13) and (15) form four simultaneous equations that may be solved for the unknowns u_1, u_2, u_4 and p_I provided one assigns values for K and C_p. The method used to solve these equations is described in the Appendix; the estimation of values for K and C_p, based on a 500 mm square Windcatcher™, is addressed in Section 3. Note that it is possible for the flow to reverse if the buoyancy force is greater than the pressure force due to the wind and under these circumstances a steady state would no longer exist. The conditions under which this occurs depends on many parameters and it will be seen in the results that follow that flow reversal is not seen to occur for $\theta = 0°$.

2.2. Unsealed room

If air exchange between the room and the surroundings (other than through the Windcatcher™) is allowed then the analysis of the previous section simplifies considerably because air exchange will set $p_I = 0$. This allows Eqs. (11)-(13) to be solved directly, noting that if the flow reverses in quadrant 1 then $\dot{Q}_I = 2u_2 A_2 + u_4 A_4 + u_1 A_1$ and

13

$$u_1 = \sqrt{\frac{gz_I[1-T_E/T_I]-2C_{p_1}u_w^2}{K_1[1+T_E/T_I]}} \,, \qquad \text{when} \quad u_w < \sqrt{\frac{gz_I}{2C_{p_1}}\left[1-\frac{T_E}{T_I}\right]}. \qquad (16)$$

Here, a steady state is maintained by air infiltration into the room.

2.3. Wind incident at $\theta = 45°$

Values of $\theta = 0°$ and $\theta = 45°$ represent limiting cases for the incident wind and so $\theta = 45°$ is reviewed in this section. When the wind is incident at $\theta = 45°$ it is assumed to enter through quadrants 1 and 2, and to extract through quadrants 3 and 4. The energy carried by the wind now splits equally between the two inlet quadrants and so Eqs. (11)-(13) are re-written to give

$$\frac{1}{2}\bar{\rho}u_{1,2}^2 K_{1,2} = \frac{1}{4}\rho_E u_w^2 C_{p_{1,2}} - \frac{gz_I p_E}{R}\left(\frac{1}{T_E}-\frac{1}{T_I}\right) - p_I \qquad (17)$$

and

$$\frac{1}{2}\bar{\rho}u_{3,4}^2 K_{3,4} = p_I + \frac{gz_E p_E}{R}\left(\frac{1}{T_E}-\frac{1}{T_I}\right) - \frac{1}{2}\rho_E u_w^2 C_{p_{3,4}}. \qquad (18)$$

Here, the inlet quadrants 1 and 2, and the outlet quadrants 3 and 4, are assumed to be identical. For a sealed room, mass continuity yields

$$\dot{Q}_1 = \dot{Q}_4. \qquad (19)$$

The symmetry that appears for $\theta = 45°$ allows Eqs. (17)-(19) to be solved analytically, giving

$$u_3 = u_4 = \sqrt{\frac{u_w^2[C_{p_1}-2C_{p_4}]-gL[1-T_E/T_I]}{[1+T_E/T_I][K_1(A_4/A_1)^2 + K_4]}}. \qquad (20)$$

Note that flow reversal will occur when

$$u_w < \sqrt{\frac{gL[1-T_E/T_I]}{[C_{P_1}-2C_{P_4}]}} \ .$$
(21)

Under these circumstances a steady state would no longer exist and so these conditions are not considered in the following section.

For an unsealed room, setting $p_I = 0$ allows Eqs. (17) and (18) to be solved directly, noting that if the flow reverses in quadrant 1 then $\dot{Q}_I = 2u_4 A_4 + 2u_1 A_1$ and

$$u_1 = u_2 = \sqrt{\frac{gz_I[1-T_E/T_I]-C_{p_1}u_w^2}{K_1[1+T_E/T_I]}} \qquad \text{when} \quad u_w < \sqrt{\frac{gz_I}{C_{p_1}}\left[1-\frac{T_E}{T_I}\right]} \ .$$
(22)

3. Semi-empirical model

The model developed in the previous section will compute ventilation rates generated by a Windcatcher™ provided one knows values for C_p and K. The C_p values are related to the design of the top section of the Windcatcher™ and the K values to the losses inside the Windcatcher™ itself. The C_p values are assumed here to depend only on wind direction, whereas the K values are assumed to be independent of wind direction. Accordingly, it is preferable to obtain these values under controlled conditions and Parker and Teekeram [11] measured C_p values for a 500 mm square Windcatcher™ in a wind tunnel, with a sealed room of volume 15.25 m^3. Elmualim [12] also used a wind tunnel to measure C_p values and this data was compared with CFD predictions. A comparison between the C_p

15

values measured by Parker and Teekeram, and Elmualim, are shown in Table 1, for $\theta = 0°$. Here, the C_p values agree well for quadrant 1, although significant discrepancies between prediction and measurement are observed for the other quadrants. The measured data does, however, agree reasonably well for the other quadrants (apart from a seemingly erroneous value in Elmualim's data for quadrant 3) and this data seems to be sufficiently consistent to provide confidence when taking an average C_p value for each quadrant.

The only C_p data available for $\theta = 45°$ is reported by Elmualim [12] for a 500 mm square Windcatcher™. Here, Elmualim compared measurements with predictions obtained using CFD and reported varying levels of agreement. In view of the discrepancies between prediction and experiment observed for $\theta = 45°$, it appears sensible here to follow the method used for $\theta = 0°$ and to use only the measured data for estimating C_p values. Moreover, Elmualim's measured data is asymmetric and this is inconsistent with the geometry of the problem and so for the calculations that follow an average value for C_p is generated for the inlet and outlet quadrants. The values used here for C_p are summarised in Table 2.

After assigning values for C_p it is necessary to identify appropriate values for the loss coefficients. One could, of course, estimate these values using, for example, standard values published by CIBSE [19]. This approach is, however, likely to lead to errors and it is arguably more consistent first to use experimental data measured over the whole Windcatcher™, before attempting to analyse individual components. The wind tunnel measurements of Elmualim and Awbi [5], and also Elmualim and Teekaram [20], provide data for flow rates into and out of a 500 mm square Windcatcher™ under controlled

conditions. Accordingly, a semi-empirical model is developed here by comparing the

predictions obtained using the model presented in the previous section with wind tunnel

measurements, and successively altering values of K until acceptable agreement is found.

In this way, the empirical data obtained under controlled conditions is being used solely to

identify the losses in the Windcatcher™; the K values calculated for a 500 mm square

Windcatcher™ are then assumed to be valid over a much wider range of conditions

applicable to real installations.

The data measured by Elmualim and Awbi [5] was obtained with a sealed room and is

presented in Fig. 2 for a Windcatcher™ with $L = 1\,\mathrm{m}$ and $d_1 = d_2 = 0.5\,\mathrm{m}$. Here, $\theta = 0°$

and the volume flow rate in each quadrant is plotted against incident wind speed for a

Windcatcher™ in which the damper and grill have been omitted. For $\theta = 0°$ the C_p

values in Table 2 are used and values for K_1, K_2 and K_4 are successively altered until

acceptable agreement between theory and experiment is achieved for the gradient m, where

$m = \dot{Q}/u_w$, assuming that a straight line passing through the origin may be used. The so-

called semi empirical predictions are compared with Elmualim and Awabi's data in Fig. 2,

with $K_1 = 3.89$ and $K_2 = K_4 = 8.44$; a comparison between measured and predicted

values for m are shown in Table 3. Here, it is evident that it is possible to vary values for

K until very good agreement between prediction and measurement is obtained (error of

less than 7%). The value of K for the inlet quadrant appears to be plausible (for example, a

simple opening equates to a value of $K = 2.7$ [15]), although one would expect the

Windcatcher™ to impart more resistance to flow than a simple opening and so a value of

$K_1 = 3.89$ appears to be reasonable. The value of K chosen for the outlet quadrants is,

however, much higher and the reasons for this are more uncertain. This value of K does,

of course, depend on the accuracy of the experimental measurements and it is possible that experimental errors may significantly affect the outlet K values, see for example the discussion on measurement errors by Elmualim [20]. Alternatively, there may also be physical reasons for increases in the outlet flow losses, for example additional losses may occur in the outlet quadrants because of the lower flow velocities in these quadrants, which are more prone to lie in the transition flow region. Moreover, increased losses may be attributable to the flow into the room interfering with the exhaust flow, which serves to increase the resistance experienced by the flow leaving the room.

The measurements taken by Elmualim and Awbi [5] were obtained with a sealed room and it is reported that more air flows into the room than flows out; the results of Parker and Teekeram [11], also for a sealed room, indicate the opposite effect. Clearly, in both studies mass is not balanced, implying mass transfer with the surroundings or, perhaps more likely, errors in the experimental measurements. The semi-empirical model developed here must balance mass and so it is interesting to view the effect this has on the predicted pressure in the room, p_I. In Fig. 3, p_I is plotted against u_w for the Windcatcher™ studied in Fig. 2 and p_I is seen to be negative for all wind speeds so that the Windcatcher™ is drawing more air from the room than is being supplied causing the pressure of the air in the room to drop, albeit only by a relatively small amount.

The results presented in Fig. 2 are for experimental data measured in the absence of a damper and grill (see Fig. 1b). Elmualim [21] later obtained data for a 500 mm square Windcatcher™ that includes both a damper and a grill and these results are presented in Fig. 4. A comparison between the experimental data in Figs. 2 and 4 shows that the losses in quadrant 1 increase by approximately 18%, which is assumed here to be attributable

18

solely to the dampers and grill. Accordingly, the values used here for K are modified to include the dampers and grill (the details of this modification is discussed in Section 3.1), giving values of $K_1 = 4.59$ and $K_2 = K_4 = 9.14$. The semi-empirical predictions obtained using these new values are compared with Elumalim's measured data in Fig. 4. Again, good agreement is observed for quadrants 1 and 4 (error of less than 11%), although for quadrant 2 an over prediction of the flow rate is evident (error of 42%).

3.1. Identification of Windcatcher™ loss factors

The values inferred for K in the previous section are for a 500 mm square Windcatcher™ as a whole and so do not provide information on those losses attributable to individual components of the Windcatcher™ apart from the estimation that the dampers and grill contribute to 18% of overall losses. Here, the measurements of Parker and Teekeram [11] are useful since they isolate the losses in the top section of the Windcatcher™ (length L_T in Fig. 1b). Parker and Teekeram measured a 500 mm square Windcatcher™ and used a fan to blow air into and out of the top section, which contains the louvers. Their data may readily be used to find the loss coefficient for the top section and this gives values of $K = 1.5$ for flow into the room, and $K = 1.32$ for flow out of the room. Identifying appropriate values for other elements of the Windcatcher™ is rather more difficult, as one must rely on estimations based on standard values. Here, estimated K values are reported in Table 4, assuming that values for the damper and grill make up 18% of the overall losses. The frictional losses have been estimated from standard data for circular ducts, and so a hydraulic diameter (d_H) is used for the (triangular) quadrants. The "additional losses" in Table 4 represent a departure from the standard losses in order to meet the overall values of K identified earlier. Following the discussion outlined earlier these additional

losses are attributed to friction losses in the quadrant and to entrance losses for the outflow quadrants. Clearly, there is an element of guesswork involved in Table 4 and more experimental/modelling work is required to shed further light on this data and also to investigate why it is necessary to assign higher values of K to the outlet quadrants.

4. Results

The semi-empirical model developed in the previous section is now applied to different scenarios in order to investigate its accuracy. For a 500 mm square Windcatcher™ identical to the one studied by Elmualim [12], Li and Mak [16] generated CFD predictions for $\theta = 0°$, $\theta = 15°$, $\theta = 30°$ and $\theta = 45°$. Li and Mak quantified air flow rates into and out of a sealed room and a comparison between their CFD predictions and those obtained using the semi-empirical model is presented in Fig. 5 (with $d_1 = d_2 = 0.5\,\text{m}$ and $L = 1\,\text{m}$). Here, good agreement is observed for $\theta = 0°$ (error of 3%), and for $\theta = 45°$ agreement is still acceptable (error of 21%). Note here that the semi-empirical predictions for $\theta = 45°$ are obtained using those K values generated for $\theta = 0°$. Elmualim and Teekeram [20] also examined the performance of a 500 mm square Windcatcher™ with $\theta = 45°$, but they obtained experimental measurements and a comparison between this data and the semi-empirical model is shown in Fig. 6. Some scattering and a lack of symmetry is evident in the experimental data, although this is likely to be caused by experimental error. The semi-empirical predictions do, however, deliver a relatively good fit for the experimental data, with an error of 3.8% if one compares the gradient of the semi-empirical predictions with a gradient based on data regression of all of the experimental data.

Elmualim [21] measured the influence of density changes by placing an electric heater in a (sealed) room and measuring the effect this had on Windcatcher™ flow rates. Elmualim generated a $10°$ temperature difference between the room and the surroundings and in Fig. 7 the semi-empirical model is compared with Elmualim's data for $\theta = 0°$ (with $T_{in} = 20°\,C$). Here, good agreement with measured data is observed for quadrants 1 and 4, with an average error of 9% and 11% for quadrants 1 and 4, respectively, although an over prediction is observed for quadrant 2 (average error of 52%). It is noticeable, however, that the semi-empirical model predicts that the change in density has little influence on the performance of the Windcatcher™. This is thought to be because the room is sealed and, in order to maintain mass continuity, the pressure of the air drops in order to compensate for the temperature change, rather than the air velocities within the Windcatcher™ changing. This effect can be observed in Fig. 8, where the pressure in the room is seen to drop as the temperature difference increases.

The predictions presented so far have been compared to data obtained under controlled conditions for a sealed room; however, in real applications the Windcatcher™ is likely to be operating in a room that allows air exchange (however small) with the surroundings, which may include adjoining rooms or surroundings external to the building. In Figs. 9 and 10 predictions are presented for flow rates in a unsealed room for a 500 mm square Windcatcher™ that is identical to the one used in previous calculations (including a damper and grill). Here, data is presented with and without a temperature difference between the room and the surroundings, and a reversal of flow in quadrant 1 is signified by a change in sign for the velocity. It can be seen that a temperature change of $3°\,C$ (with

21

$T_{in} = 25°\,\mathrm{C}$) only significantly alters Windcatcher™ performance at low wind speeds, where a reversal of the flow in quadrant 1 is observed. This effect is, however, more noticeable for $\theta = 45°$ and the flow in quadrant 1 is seen to reverse at a higher wind velocity when compared to $\theta = 0°$. This is thought to be because the Windcatcher™ is less efficient at gathering the incident energy from the wind when $\theta = 45°$ and so the buoyancy of the air is larger relative to the wind energy. It is interesting also to compare the outlet volume flow rates for the unsealed room with those found previously for a sealed room. In Table 5, the gradient (m) of $\dot{Q}$ vs u_W is compared for $\theta = 0°$ and $\theta = 45°$. Here, it is evident that the results for the sealed and unsealed rooms are similar and that for $\theta = 0°$ the model is predicting that more air will flow out of the room when the room is unsealed. When $\theta = 45°$ the air flow rate from the room clearly drops when compared to $\theta = 0°$, as one would expect; however, it is seen that the sealed room now produces the largest flow rate, which is the opposite to that seen for $\theta = 0°$. It is not clear here why this should be the case when $\theta = 45°$.

There is very little data in the literature that quantifies the ventilation performance of a Windcatcher™ working *in situ*. Clearly, accurately measuring parameters such as wind speed and air velocity inside Windcatcher™ quadrants presents a number of difficulties. Data has, however, been published by Kirk and Kolokotroni [14] for Windcatchers™ similar to those studied here, but operating in an open plan office environment. Kirk and Kolokotroni measured air exchange rates and published a plot of the volume flow rate of the air expelled from the office versus wind speed, making this data suitable for comparison with the current study. The office studied by Kirk and Kolokotroni contained four Windcatchers™ and data is reported for the first floor of the office, which contained

two Windcatchers™ of dimensions 1.2 m square and two that were 0.6 m square, although

Kirk and Kolokotroni note that only half of each Windcatcher™ serves the first floor,

whilst the other half serves the ground floor. Accordingly, they propose that this

arrangement effectively behaves as one 1.2 m square and one 0.6 m square Windcatcher™

serving the first floor. The accuracy of this assumption is debatable, but their measured

data does provide an opportunity to review the accuracy of the semi-empirical model under

what are far from idealised conditions, and also to examine the feasibility of extrapolating

a semi-empirical model based on 500 mm square Windcatcher™ data to other geometries.

Accordingly, in Fig. 11 the semi-empirical predictions are compared with Kirk and

Kolokotroni's data assuming a temperature difference of $5°$ C between the room and the

surroundings (with $T_{in} = 20°$ C). The predictions in Fig. 11 were obtained for a

Windcatcher™ containing a damper and grill in an unsealed room, and by summing the

volume flow rates calculated separately for a 1.2 m square and a 0.6 m square

Windcatcher™. It is evident in Fig. 11 that the predictions for $\theta = 45°$ compare very well

with experimental measurements (an average error of 12%), although one may argue here

that this level of agreement is somewhat fortuitous and that the wind direction varied when

the measurements were taken and so cannot be assumed to be exactly $\theta = 45°$. However,

these results demonstrate that there is some promise in using C_p and K values determined

for a 500 mm square Windcatcher™ to predict the performance of Windcatchers™ of

other dimensions. It should be observed also that the "theoretical" model used by Kirk and

Kolokotroni that delivers good agreement with the experimental data contains at least two

heuristic constants with little supporting justification; moreover, there is no guide as to

how transferable these constants are and how they should be applied to different

applications, therefore it is doubtful that they reflect the true physics of the problem.

Furthermore, given the experimental errors likely to be present in the semi-empirical model and the experimental data, one cannot expect excellent agreement between prediction and measurement and so the semi-empirical model must be treated only as an estimate of true Windcatcher™ performance. Nevertheless, the predictions obtained for $\theta = 0°$ and $\theta = 45°$ both lie within a reasonable distance of the experimental data and it appears sensible here to treat these predictions as limiting cases, where $\theta = 0°$ represents an estimate of optimum performance and $\theta = 45°$ an estimate of a worst case performance.

In Section 3 the estimated losses in an outlet quadrant were seen to be significantly higher than those in the inlet quadrants. This is of some concern, especially for an unsealed room. In Table 6, the gradient m is plotted for differing values of $K_{2,4}$ and the effect this has on the predicted volume flow rates from an unsealed room (for a 500 mm square Windcatcher™ with dampers and grill) is investigated. Here, it is evident that, as one reduces the value of $K_{2,4}$ the volume flow rate increases, as one would expect. The lower limit chosen here is $K_{2,4} = K_1$ and the flow rates predicted at this limit are 40% higher than those seen when $K_{2,4} = 9.14$. This represents a significant difference when the room is unsealed and so in the future more experimental data is necessary in order to be confident of the values estimated here for the outlet loss coefficients. In particular it is important to investigate these values under real operating conditions, as it may be possible that the K values used here are unduly influenced by those laboratory conditions under which the measurements took place, and that these do not reflect the true behaviour of the Windcatcher™ *in situ*.

Finally, the ultimate aim here is to deliver a simple method for estimating the ventilation rate delivered by a Windcatcher™. If one neglects the effects of air buoyancy, which has previously be shown to be significant only at low wind speeds, then it is obvious that a simple linear relationship is predicted between the Windcatcher™ volume flow rate and the wind speed. This makes parametric studies and the collapsing of data into simple expressions very straightforward. Accordingly, the volume flow rates for a number of square Windcatchers™ of different dimensions, in which a damper and grill are present for an unsealed room, have been computed for $\theta = 0°$ and $\theta = 45°$. From these calculations, the following simple expressions can be obtained:

$$\dot{Q}_{out} = 0.1251\, A u_w \qquad \text{for} \qquad \theta = 0° \qquad\qquad (23)$$

and

$$\dot{Q}_{out} = 0.0747\, A u_w \qquad \text{for} \qquad \theta = 45°. \qquad\qquad (24)$$

Here, $\dot{Q}_{out}$ is the volume flow rate of air removed by the Windcatcher™ from an unsealed room, A is the cross-sectional area of the whole Windcatcher™ (i.e. $A = A_1 + A_2 + A_3 + A_4$), and u_w is the incident wind speed. These equations neglect buoyancy effects and are for a Windcatcher™ of length $L = 1\,\text{m}$. According to the model used here the effect of changing the length of the Windcatcher™ on the curves is small, for example increasing the length of the Windcatcher™ to 10 m lowers the constant in Eq. (23) by only 5%; however, it should be stressed here that the semi-empirical model is based on measurements taken for a relatively short Windcatcher™ and it is assumed that one may simply scale up the frictional losses for longer duct length; the accuracy of this assumption remains to be tested for longer Windcatchers™ that, say, operate over a number of floors. Furthermore, Eqs. (23) and (24) assume that the C_p and K values

obtained for a 500 mm square Windcatcher™ may be applied to other geometries (through the area A). The validity of this assumption was investigated in Fig. 11, where good agreement was observed; however, it is also possible to compare these expressions with the results of Hughes and Ghani, who used CFD to predict the ventilation rates for a 1000 mm square top-down ventilation device similar to the Windcatcher™ being studied here. If a regression analysis is undertaken for the linear region of Hughes and Ghani's CFD predictions for "counter current flow", one obtains the expression $\dot{Q}_{out} = 0.116\,u_w$. For a 1000 mm square Windcatcher™, Eq. (23) gives $\dot{Q}_{out} = 0.1251\,u_w$, which is very close to the relationship predicted by Hughes and Ghani and further validates the semi-empirical expressions derived here. Thus, the semi-empirical model derived using data for 500 mm square Windcatchers™ provides good agreement with two studies in which the geometry of the device is altered. This provides confidence in the use of Eqs. (23) and (24) over a range of geometries, although it would be sensible here to gather further experimental data for different geometries, preferably under controlled conditions, in order to further establish the accuracy of these equations. Furthermore, it appears sensible to view Eqs. (23) and (24) as an estimation of the upper and lower limits of Windcatcher™ performance, recognising that they are derived from a semi-empirical model and that, by definition, these equations will contain experimental errors and so should be treated only as an estimation of true Windcatcher™ performance.

5. Conclusions

A semi-empirical model is developed here that combines a simple analytic model with experimental data reported in the literature. The model draws on data measured for the coefficient of pressure on each face of a 500 mm square Windcatcher™, and then infers losses in each Windcatcher™ quadrant from measurements of ventilation rates. A semi-empirical model is developed here in the belief that this is the only practical approach to quickly and accurately estimating Windcatcher™ performance, especially in view of the highly turbulent nature of the flow round a typical Windcatcher™ and the problems this has been seen to cause for numerical models; however, this approach means that any errors present in the experimental measurements will also appear in the model and so such a model can only be as good as the experimental data available. Moreover, the experimental data utilised here was obtained under laboratory conditions for a 500 mm square Windcatcher™ in a sealed room and so an assumption inherent in this approach is that this data may be extrapolated to real, *in situ*, applications in which air transfer between the room and the surroundings is permitted and different Windcatcher™ geometries are present.

The loss coefficients used in the semi-empirical model allow very good agreement to be obtained between the model and experimental data; however, the loss coefficient necessary to obtain good agreement for the extract ducts was much higher than for the supply duct and it is not entirely clear why this should be the case. It is possible that increased frictional effects and interference effects between the supply and extract flows can explain this increase, although further experimental investigation is required in order to be certain of the cause. After assigning the empirical constants the model was compared against

other experimental and theoretical data and good agreement is generally observed for different wind directions. Air buoyancy was also analysed and here the effects of buoyancy on the performance of a Windcatcher™ were observed to be significant only at wind speeds below approximately 1 m/s for wind of normal incidence. When the wind changes direction the relative effect of the buoyancy forces increases and for an angle of incident of 45° buoyancy becomes significant at higher wind speeds, although this effect is still small above approximately 2 m/s. Accordingly, the results presented here appear to indicate that for temperature differences of less than 10° C, the effects of buoyancy may be neglected for wind speeds greater than about 2 m/s.

The semi-empirical model was also validated against *in situ* measurements of Windcatcher™ performance and here excellent agreement with measured data is observed, although this required certain assumptions about wind direction, and the level of agreement is, probably, rather fortuitous. The semi-empirical model has, however, been shown to perform well against a range of experimental data and CFD predictions, and so offers the potential for use as a quick iterative design tool. To this end, a very simple expression for extract ventilation rates is proposed that, after neglecting buoyancy effects, provides a very quick estimate of Windcatcher™ performance that requires no computational effort.

Acknowledgement

Appendix

Equations (11)-(13) and (15) can only be solved iteratively and it is common for this type
of problem to successively change p_I until Eq. (15) is satisfied. This method is, however,
rather cumbersome and it is more efficient to use a recognised root finding technique,
which will deliver a much faster method that is easily automated. Here, the Newton
Raphson method is adopted and Eqs. (11)-(13) and (15) are first combined to give

$$f_1(u_2, u_4) = u_2^2 + \left(\frac{A_4}{A_2}\right) u_2 u_4 + a_4 u_4^2 + b_4 \tag{A1}$$

and

$$f_2(u_2, u_4) = u_4^2 + 4\left(\frac{A_2}{A_4}\right) u_2 u_4 + a_2 u_2^2 + b_2. \tag{A2}$$

The constants a_2 and a_4 are given by

$$a_2 = 4\left(\frac{A_2}{A_4}\right)^2 + \frac{K_2}{K_1}\left(\frac{A_1}{A_4}\right)^2 \tag{A3}$$

and

$$a_4 = \frac{1}{4}\left(\frac{A_4}{A_2}\right)^2 + \frac{K_4}{4K_1}\left(\frac{A_1}{A_2}\right)^2. \tag{A4}$$

The constants b_2 and b_4 are given by

$$b_2 = \frac{1}{K_1[1+T_E/T_I]}\left(\frac{A_1}{A_4}\right)^2 \left\{2(C_{p_2} - C_{p_1})u_w^2 - gL[1-T_E/T_I]\right\} \tag{A5}$$

and

$$b_4 = \frac{1}{4K_1[1+T_E/T_I]}\left(\frac{A_1}{A_2}\right)^2 \left\{2(C_{p_4} - C_{p_1})u_w^2 - gL[1-T_E/T_I]\right\}. \tag{A6}$$

In general, $\mathbf{u} = [u_2 \quad u_4]^{\mathrm{T}}$, $\mathbf{f} = [f_1 \quad f_2]^{\mathrm{T}}$ and the Newton Raphson method gives

$$\{\overline{\mathbf{u}}\} = \{\mathbf{u}\} - [\mathbf{J}]^{-1}\{\mathbf{f}\} . \tag{A7}$$

Here, $\mathbf{u}$ is an initial guess and $\overline{\mathbf{u}}$ is the new solution found after solving the right hand

side of Eq. (A7). The Jacobian $[\mathbf{J}]$ is given by

$$[\mathbf{J}] = \begin{bmatrix} 2u_2 + u_4 A_4 / A_2 & u_2 A_4 / A_2 + 2a_4 u_4 \\ 4u_4 A_2 / A_4 & 2u_4 + 4A_2 u_2 / A_4 \end{bmatrix} . \tag{A8}$$

This method requires the identification of an initial guess for $\mathbf{u}$. When $\theta = 0^\circ$ the

velocities in quadrant 4 are relatively small when compared to the other quadrants and so

for an initial guess it appears sensible first to assume that $u_4 \rightarrow 0$, which gives

$\mathbf{u} = [\sqrt{b_4} \quad 0]$. On solving Eq. (A7) for u_2 and u_4 it is then straightforward to return to

Eq. (15) to find u_1, and Eq. (13) to find p_I. For subsequent calculations for different

values of u_w it is sensible to use values for $\mathbf{u}$ calculated for a previous (preferably lower)

value of u_w as an initial guess.

30

References

1   Beazley E, Harverson M. Living with the Desert: Working Buildings of the Iranian Plateau, Orchid Press, Thailand 1982.

2   Montazeri H, Azizian R. Experimental study on natural ventilation performance of one-side wind catcher. Building and Environment 2008; 43(12): 2193-2202.

3   Khan N, Su Y, Riffat SB. A review on wind driven ventilation techniques. Energy and Buildings 2008; 40(8): 1586-1604.

4   Gage SA, Graham JMR. Static split duct roof ventilators. Building Research & Information 2000; 28(4): 234-244.

5   Elmualim AA, Awbi HB. Wind Tunnel and CFD Investigation of the Performance of Windcatcher Ventilation Systems. International Journal of Ventilation 2002; 1(1): 53-64.

6   Etheridge D, Sandberg M. Building Ventilation: Theory and Measurement, Wiley, UK 1996.

7   Etheridge, D. Natural Ventilation through Large Openings - Measurements at Model Scale and Envelope Flow Theory. International Journal of Ventilation 2004; 2(4): 325-342.

8   CIBSE. Natural Ventilation in Non-Domestic Buildings AM10, 2005.

9   Liddanet MW, A Guide to Energy Efficient Ventilation, Air Infiltration and Ventilation Centre, Oscar Faber, 1996.

10   Santamouris M, Asimakopoulos D. Passive Cooling of Buildings, Earthscan, 1996.

11   Parker J, Teekeram AJ. Design and Application Guide for Roof Mounted Natural Ventilation Systems. BSRIA, UK 2004.

12 Elmualim AA. Dynamic modelling of a wind catcher/tower turret for natural ventilation. Building Services Engineering Research and Technology 2006; 27(3): 165-182.

13 Su Y, Riffat SB, Lin Y-L, Khan N. Experimental and CFD study of ventilation flow rate of a Monodraught™ windcatcher. Energy and Buildings 2008: 40(6): 1110-1116.

14 Kirk S, Kolokotroni M. Windcatchers in Modern UK Buildings: Experimental Study. International Journal of Ventilation 2004; 3(1): 67-78.

15 Shea AD, Robertson AP, Aston WI, Rideout NM. The performance of a roof-mounted natural ventilator. 11th International Conference on Wind Engineering. Texas Tech University, Lubbock, Texas, USA 2003.

16 Li L, Mak CM. The assessment of the performance of a Windcatcher system using computational fluid dynamics. Building and Environment 2007; 42(3): 1135-1141.

17 Hughes BR, Ghani SAA. A numerical investigation into the effect of windvent dampers on operating conditions. Building and Environment 2009; 44(2): 237-248.

18 Hughes BR, Ghani SAA. Investigation of a windvent passive ventilation device against current fresh air supply recommendations. Energy and Buildings 2008: 40(9): 1651-1659.

19 CIBSE. Guide C 2001.

20 Elmualim AA, Teekaram AJ. Natural Ventilation Testing Carried out for Monodraught Ltd., BSRIA, UK 2002.

21 Elmualim AA. Effect of damper and heat source on wind catcher natural ventilation performance. Energy and Buildings 2005; 38(8): 939-948.
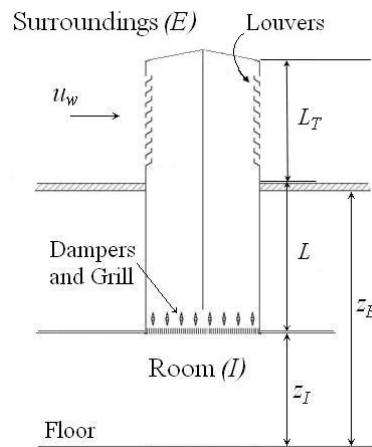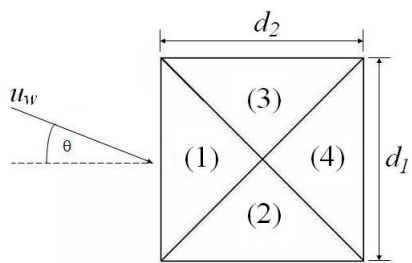
Figure 1a. Plan view of Windcatcher™.   Figure 1b. Side view of Windcatcher™.
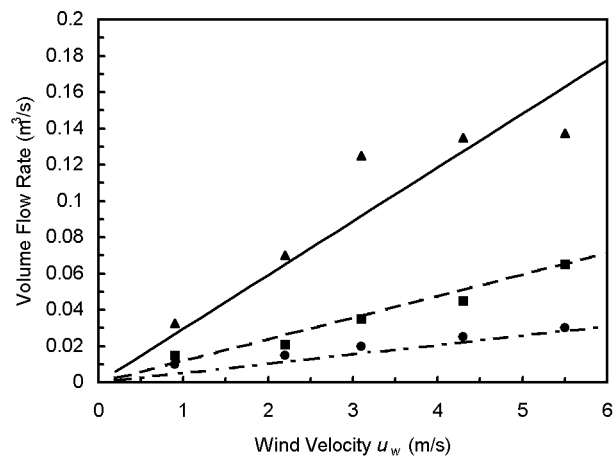
Figure 2. Comparison between semi-empirical predictions and the experimental measurements of Elmualim and Awbi [5] without dampers and grill for $\theta = 0°$. Quadrant 1, ——— , prediction, ▲ , experiment; quadrant 2, — — — , prediction, ■ , experiment; quadrant 4, — - — - — , prediction, ● , experiment.
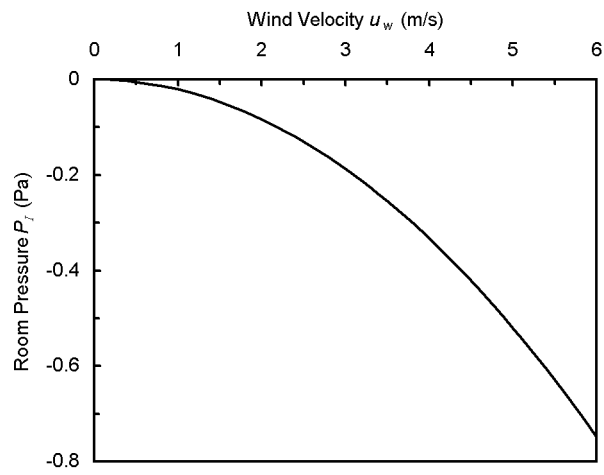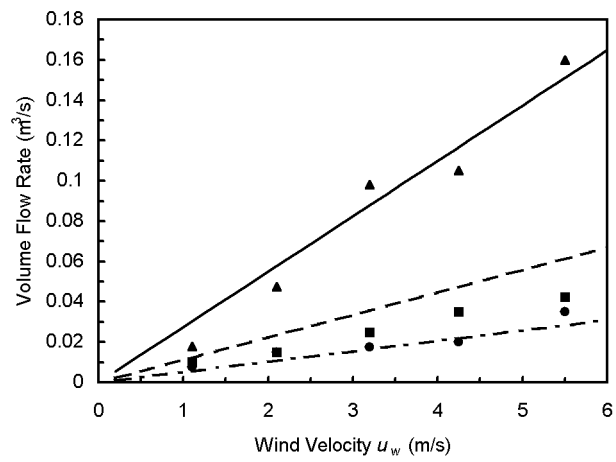
Figure 3. Predicted pressure in a sealed room without dampers and grill for $\theta = 0°$.

Figure 4. Comparison between semi-empirical predictions and the experimental measurements of Elmualim [21] with dampers and grill for $\theta = 0°$. Quadrant 1, ——— , prediction, ▲ , experiment; quadrant 2, — — — , prediction, ■ , experiment; quadrant 4, — - — - — , prediction, ● , experiment.
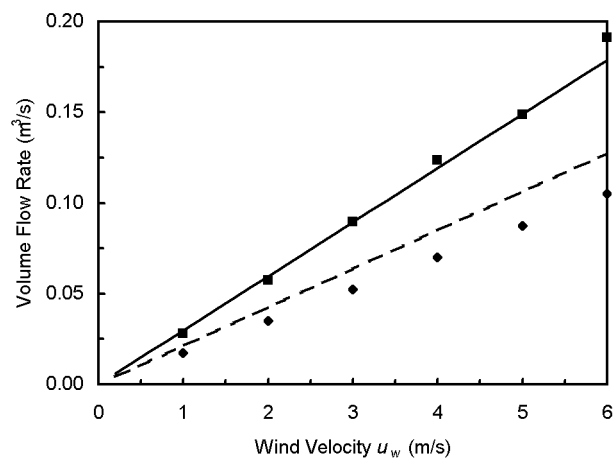
Figure 5. Comparison between semi-empirical predictions and the CFD predictions of Li and Mak [16] for ventilation rates from a sealed room, without dampers and grill. $\theta = 0°$, ———— , semi-empirical model, ■ , CFD; $\theta = 45°$, — — — , semi-empirical model, ● , CFD.
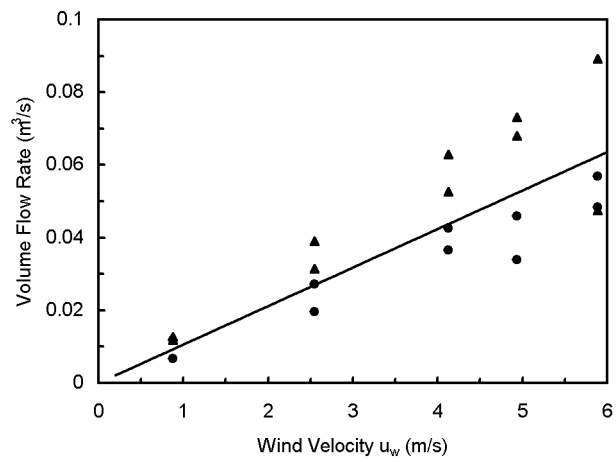
Figure 6. Comparison between semi-empirical predictions and the experimental measurements of Elmualim and Teekaram [20] for ventilation rates from a sealed room, without dampers and grill. $\theta = 45°$, ———— , prediction, ▲ and ●, experiment.
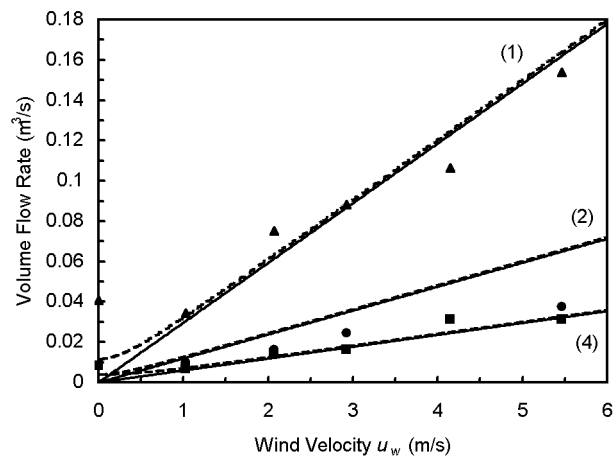
Figure 7. Comparison between semi-empirical predictions and the experimental measurements of Elmualim [21] without dampers and grill for $\theta = 0^\circ$. Labelled quadrants, ———, prediction $\Delta T = 0^\circ\text{C}$, — — —, prediction $\Delta T = 10^\circ\text{C}$. Experiment: ▲, quadrant 1; ●, quadrant 2; ■, quadrant 4.
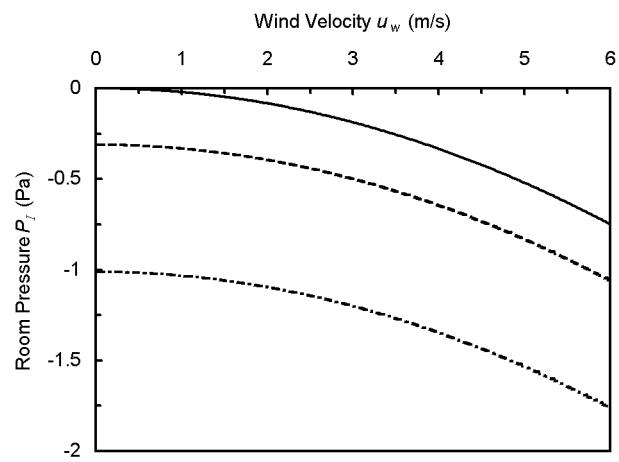
Figure 8. Predicted pressure in unsealed room. ———— , $\Delta T = 0^{\circ}\mathrm{C}$; — — — , $\Delta T = 3^{\circ}\mathrm{C}$, — · — · — , $\Delta T = 10^{\circ}\mathrm{C}$.
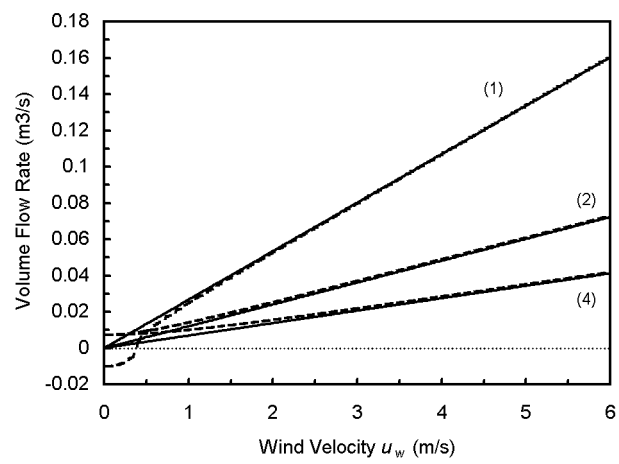
Figure 9. Predictions for unsealed room for $\theta = 0°$. Labelled quadrants, ——— , prediction $\Delta T = 0°\text{C}$, — — — , prediction $\Delta T = 3°\text{C}$.
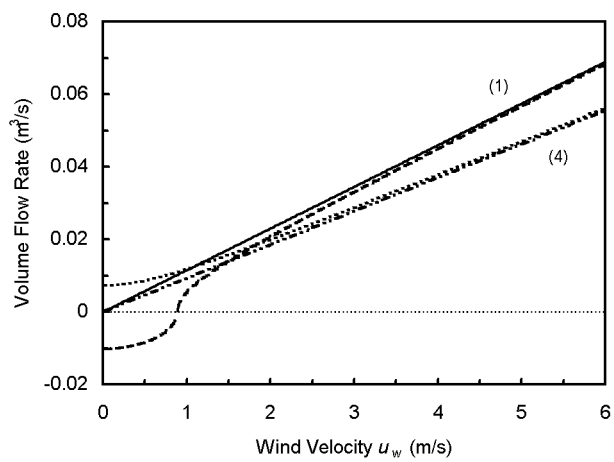
Figure 10. Predictions for unsealed room for $\theta = 45°$. Labelled quadrants, ——— , prediction $\Delta T = 0°\text{C}$, — — — , prediction $\Delta T = 3°\text{C}$.
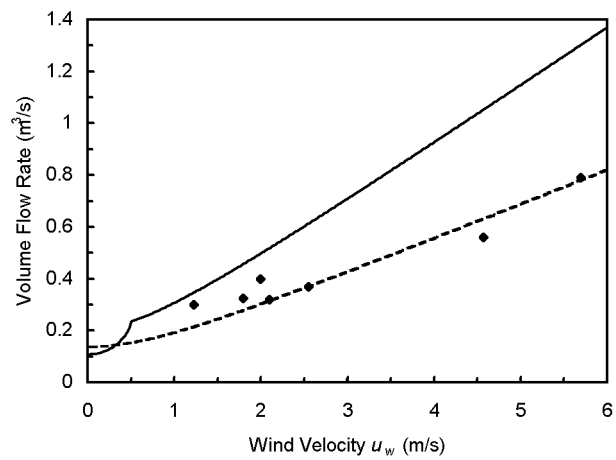
Figure 11. Comparison between semi empirical predictions and the experimental measurements of Kirk and Kolokotroni [14] for ventilation rates from an unsealed room, with dampers and grill. ——— , prediction $\theta = 0°$; — — — , prediction $\theta = 45°$; ♦ , experiment.

Table 1. C_p values for $\theta = 0°$.

Quadrant	Experiment. [11]	Experiment [12]	CFD. [12]
1	0.853	0.830	0.840
2	-0.348	-0.034	-0.550
3	-0.348	-0.330	-0.550
4	-0.116	-0.100	-0.440

Table 2. C_p values used in semi-empirical model		
	$\theta = 0°$	$\theta = 45°$
C_{p_1}	0.84	0.31
C_{p_2}	-0.34	0.31
C_{p_3}	-0.34	-0.2
C_{p_4}	-0.11	-0.2

Table 3. Gradient (m) of $\dot{Q}$ vs u_w.

Quadrant	m Damper and grill omitted			m Damper and grill included		
	Experiment [5]	Model	Error %	Experiment [21]	Model	Error %
1	0.0298	0.0298	0	0.0274	0.0277	1.1
2	0.0112	0.0119	6.3	0.0079	0.0112	41.8
3	0.0112	0.0119	6.3	0.0079	0.0112	41.8
4	0.0059	0.0060	1.7	0.0058	0.0052	10.3

Table 4. Loss coefficients for Windcatcher™

Section	Supply K_1	Extract $K_{2,4}$
Top section	1.5	1.32
Inlet	0.5	4.83
Outlet	1.0	1.0
Duct	$K_{\text{frict}}=0.06L/d_H$	$K_{\text{frict}}=0.06L/d_H$
Additional Loss	0.6	1.0
Grill	0.35	0.35
Dampers	0.35	0.35
Total	$4.3+K_{\text{frict}}$	$8.85+K_{\text{frict}}$

Table 5. Predicted gradient (m) of $\dot{Q}$ vs u_w,
damper and grill included.

Quadrant	m unsealed		m sealed	
	$\theta = 0°$	$\theta = 45°$	$\theta = 0°$	$\theta = 45°$
1	0.0267	0.0115	0.0275	0.0101
2	0.0121	0.0115	0.0112	0.0101
3	0.0121	0.0092	0.0112	0.0101
4	0.0069	0.0092	0.0051	0.0101

Table 6. Sensitivity of predicted volume flow rate to value of $K_{2,4}$	
$K_{2,4}$	Gradient m
$8.85 + K_{\text{frict}}$	0.0310
$7 + K_{\text{frict}}$	0.0347
$6 + K_{\text{frict}}$	0.0373
$5 + K_{\text{frict}}$	0.0407
K_1	0.0437